ARTICLES

Solution and Photoproperties of *N*-(2-Hydroxypropyl)methacrylamide Copolymer−Meso-chlorin e_6 Conjugates

Jane-Guo Shiah,[†] Čestmír Koňák,[†,‡] John D. Spikes,[§] and Jindřich Kopeček*[,†]

Departments of Pharmaceutics and Pharmaceutical Chemistry/CCCD and of Bioengineering, Department of Biology, University of Utah, Salt Lake City, Utah 84112, and Institute of Macromolecular Chemistry, Academy of Sciences of the Czech Republic, Heyrovsky Sq. 2, 162 06 Prague 6, Czech Republic

Received: January 29, 1997[⊗]

The solution properties of *N*-(2-hydroxypropyl)methacrylamide (HPMA) copolymers containing various numbers of meso-chlorin e_6 monoethylenediamine (Mce_6) molecules attached to the copolymer via either glycine (G) or tetrapeptide (GFLG) side chains were studied. Dynamic light scattering, spectroscopic, fluorescence quenching, and time-resolved fluorescence techniques were used. The photosensitizing efficiencies of the various derivatives were also examined. Reactions were measured in aqueous sodium phosphate buffer (SPB) and ethanol. The dynamic light scattering data indicate that the intermolecular aggregation of Mce_6 species within the HPMA copolymer conjugates is not important at the conjugate concentration measured (5×10^{-4} g/mL). However, intramolecular aggregation of the hydrophobic Mce_6 moieties does occur and was studied using absorption and fluorescence techniques. The degree of intramolecular aggregation was decreased by the addition of detergents or ethanol to the SPB solutions. The cationic detergent, CTAB, strongly enhanced the fluorescence of the copolymer conjugates due to its efficient electrostatic interactions with the negatively charged Mce_6 species. It also significantly increased the relative quantum yield of oxygen uptake during the copolymer conjugate-sensitized photooxidation of furfuryl alcohol. The observed iodide quenching of copolymer conjugate fluorescence implies that hydrophobic domains of aggregated Mce_6 moieties may exist in SPB solutions of the conjugates. The time-resolved fluorescence decay measurements showed that about 15% of the Mce_6 species were aggregated in SPB solutions of those copolymer conjugates with the highest Mce_6 content. There was a low degree of aggregation of free Mce_6 molecules in SPB solutions at the concentrations used.

Introduction

Meso-chlorin e_6 monoethylenediamine (Mce_6) has been suggested as an effective "second generation" photosensitizer candidate for photodynamic therapy.[1] It has a large extinction coefficient, a high quantum yield of triplet and singlet oxygen formation, and low dark toxicity. It absorbs in the red region of the spectrum, permitting deeper light penetration into tissues as compared to porphyrins.[1] The attachment of photosensitizers to targetable water soluble polymeric carriers may result in their localization in a subset of cells. A double targeting effect may be achieved by subsequent localization of light.[2] However, upon binding of hydrophobic moieties (photosensitizers) to side chain termini of hydrophilic polymer carriers, conjugates are obtained that possess amphiphilic properties in the aqueous phase.[3−8] The resulting intermolecular or intramolecular aggregation affects the conformation of polymer chains with concomitant changes in their therapeutic efficacy.[4,5] It was shown previously that the covalent binding of the photosensitizer, Mce_6, to a model *N*-(2-hydroxypropyl)methacrylamide (HPMA) copolymer significantly reduced the quantum yield of singlet oxygen production by illuminated Mce_6 moieties from 0.73 to 0.25.[9,10] The effect of coil collapse on the photoproperties of macromolecules was recently demonstrated on copolymers with pendant carbazole chromophores.[11] These results, as well as those obtained with a zinc(II) phthalocyanine−HPMA copolymer conjugate[12,13] and porphyrin− and phthalocyanine−polystyrene conjugates,[14] were attributed to an intensified aggregation of the photosensitizer moieties attached to the polymer carriers. We have initiated a series of detailed studies to permit a better understanding of the aggregation process of Mce_6 covalently bound to side chains of HPMA copolymers.

This paper deals with the solution, photophysical, and photosensitizing properties of HPMA copolymer−Mce_6 conjugates where the Mce_6 moieties were attached to the HPMA copolymers via amino acid (G) or tetrapeptide (GFLG) side chains. The solution properties of HPMA copolymer−Mce_6 conjugates were studied using a dynamic light scattering method to characterize the random association of the copolymer conjugates on the macromolecular and supramolecular levels. UV/vis and fluorescence spectroscopy, fluorescence quenching by iodide anion, and time-resolved fluorescence decay techniques were used to characterize Mce_6 aggregation on the segmental level. The photosensitizing efficiencies of the HPMA copolymer conjugates were also measured. Since the solvent exhibited a significant influence on the extent of Mce_6 aggregation, the effects of an organic solvent (ethanol) and a variety of detergents, including CTAB, Triton X-100, and SDS, on the

* Corresponding author: phone (801) 581-7211; fax (801) 581-7848; e-mail: jindrich.kopecek@m.cc.utah.edu.
† Departments of Bioengineering and of Pharmaceutics and Pharmaceutical Chemistry, University of Utah.
‡ Academy of Sciences of the Czech Republic.
§ Department of Biology, University of Utah.
⊗ Abstract published in *Advance ACS Abstracts,* July 15, 1997.

S1089-5647(97)00360-X CCC: $14.00

TABLE 1: Molecular Characteristics and Hydrodynamic Radii of HPMA Copolymer−Mce_6 Conjugates

conjugate	mol % Mce_6 in P-G-Mce_6	mol % Mce_6 in P-GFLG-Mce_6	$R_h{}^a(90°)^a$ (nm) SPB/ethanol
1	0.36		7.2 ± 0.2/6.3 ± 0.4
2	2.7		8.2 ± 0.2/7.0 ± 0.4
3		0.37	8.1 ± 0.2/7.9 ± 0.3
4		3.3	6.7 ± 0.3/7.8 ± 0.4

[a] The apparent hydrodynamic radius of conjugate copolymers measured at the scattering angle $\theta = 90°$.

aggregation of free Mce_6 and HPMA copolymer−Mce_6 conjugates were studied.

Experimental Section

Abbreviations: C_{MC}, critical micellar concentration; CTAB, hexadecyltrimethylammonium bromide; DLS, dynamic light scattering; DMSO, dimethyl sulfoxide; F, phenylalanine; G, glycine; HPMA, *N*-(2-hydroxypropyl)methacrylamide; HSA, human serum albumin; L, leucine; MA, methacryloyl; Mce_6, meso-chlorin e_6 monoethylenediamine; M_n, number-average molecular weight; M_w, weight-average molecular weight; ns, nanosecond; ONp, *p*-nitrophenoxy; P, *N*-(2-hydroxypropyl)-methacrylamide copolymer backbone; SDS, sodium dodecyl sulfate; SPB, sodium phosphate buffer; Triton X-100, (*tert*-octylphenoxy)polyethoxyethanol.

Materials. Meso-chlorin e_6 monoethylenediamine disodium salt was obtained from Porphyrin Products, Inc., Logan, UT, and was purified on an LH-20 column (2 × 52 cm) equilibrated with methanol. CTAB, Triton X-100, SDS, and HSA were from the Sigma Chemical Co., St. Louis, MO, and were of reagent grade or higher purity. They were used as received, without further purification. Sodium phosphate buffer (SPB) was adjusted to pH 7.4 as monitored by a Corning pH meter model 340 calibrated with Corning standard buffers.

Synthesis of HPMA Copolymer Conjugates. The monomers, methacryloylglycine *p*-nitrophenyl ester (MA-G-ONp),[15] methacryloylglycylphenylalanylleucylglycine *p*-nitrophenyl ester (MA-GFLG-ONp)[16] and HPMA[17] were synthesized as described previously. The copolymer conjugate precursors, P-G-ONp (**A**) for the preparation of copolymer conjugates **1** and **2** and P-GFLG-ONp (**B** and **C**) for the preparation of copolymer conjugates **3** and **4**, respectively, were prepared by radical precipitation copolymerization of HPMA with MA-G-ONp and MA-GFLG-ONp, respectively, in acetone.[18] The HPMA copolymer conjugate precursors obtained were **A** (M_w = 15 000, M_w/M_n = 1.3), **B** (M_w = 17 000, M_w/M_n = 1.5), **C** (M_w = 19 000, M_w/M_n = 1.5), and the weight- and number-average molecular weights were determined after aminolysis with 1-amino-2-propanol by size exclusion chromatographic analysis on a Superose 6 column (1.0 × 30 cm) calibrated with fractions of poly(HPMA) (buffer 0.5 M NaCl + 50 mM Tris; pH 8). The contents of ONp groups were 10.6, 5.6, and 7.8 mol % for precursors **A**, **B**, and **C**, respectively, determined by UV spectrophotometry ($\epsilon_{275} = 0.95 \times 10^4$ M^{-1} cm^{-1} in DMSO).[19] Mce_6 was bound to P-G-ONp or P-GFLG-ONp by aminolysis of reactive ONp groups in DMSO, as described elsewhere.[10] The crude products were purified by dissolving them in methanol before applying the solutions to an LH-20 column (2 × 52 cm) equilibrated with methanol. The copolymer conjugate fractions were collected, evaporated to dryness, dissolved in distilled water, frozen, and then lyophilized. The Mce_6 content of the HPMA copolymer−Mce_6 conjugates was determined by UV spectrophotometry ($\epsilon_{394} = 1.58 \times 10^5$ M^{-1} cm^{-1} in methanol). The properties of the conjugates are listed in Table 1.

Preparation of Samples. Free Mce_6, P-G-Mce_6, and P-GFLG-Mce_6 were dissolved in methanol to give final stock solutions equivalent to 400 μM Mce_6. For experiments, appropriate aliquots of the stock solutions were placed in glass tubes and evaporated to dryness under a high vacuum. The dried Mce_6 or copolymer conjugate samples were then resuspended in appropriate amounts of buffer or solvent mixtures to give the desired Mce_6 or Mce_6 equivalent concentrations.[10]

Dynamic Light Scattering Measurements. Dynamic light scattering measurements were performed using a standard multiangle Brookhaven Instruments spectrometer provided with an argon ion laser and a 78 channel BI 2030, multibit autocorrelator (Brookhaven Instruments). The samples were thermostated in a refractive index-matching liquid (toluene). The method of cumulants, using both the measured and floating baseline options and assuming homodyne detection, was used to analyze the data. The apparent diffusion coefficients, D^a, were calculated from the characteristic decay rate, Γ (the first cumulant), using the equation

$$D^a = \Gamma/q^2 \quad (1)$$

where q is the length of the scattering vector. The apparent hydrodynamic radius, $R_h{}^a$, was calculated from the Stokes−Einstein relationship:

$$R_h{}^a = kT/6\pi\eta D^a \quad (2)$$

where k is the Boltzmann constant, T is the absolute temperature, and η is the solvent viscosity.

Absorption and Fluorescence Measurements. Absorption spectra were recorded on a Perkin-Elmer Lambda 6/PECSS spectrophotometer. The Soret band was separated into two mixed Gaussian−Lorentzian spectra by the peak deconvolution technique. Fluorescence spectra were recorded on an ISS/PC-1 photon-counting spectrofluorometer. The spectral resolution of both the excitation and emission monochromators was about 2 nm.

Relative Quantum Yield of Oxygen Uptake Measurements. A recording oxygen electrode system was used to measure the quantum yield of oxygen uptake, defined as [initial uptake rate of oxygen molecules]/[initial absorption rate of photons], during the HPMA copolymer−Mce_6 conjugate-sensitized photooxidation of furfuryl alcohol.[10,20] Furfuryl alcohol was used as a model substrate since it is transparent and miscible with aqueous buffers. It reacts efficiently with singlet oxygen but does not react with hydrogen peroxide or radicals.[21,22] A 500 W quartz−tungsten light source provided with a 398 nm band-pass filter (from Corion Corp., Holliston, MA) with a bandwidth of 10 ± 2 nm at 50% transmission, corresponding closely to the Soret peaks of the HPMA copolymer−Mce_6 conjugates, was used for illumination. Incident light fluence rates were approximately 3 mW/cm^2.[10,20] The error in the quantum yield measurements was approximately ±10%. Photooxidation measurements were carried out at 25 °C in air-saturated solutions (0.22 mM oxygen). Reaction mixtures were in 20 mM SPB at pH 7.4 and contained quantities of HPMA copolymer−Mce_6 conjugates giving Mce_6 equivalent concentrations of 5 μM.

Fluorescence Quenching Measurements. Fluorescence quenching measurements were performed on a photon-counting spectrofluorometer (ISS/PC-1) at room temperature. The KI salt was used as a quencher. Fluorescence quenching was measured for both the free and copolymer-bound Mce_6 sensitizers as a function of KI concentration over the range 0−0.3 M at pH 7.4. The solutions were prepared by Job's method of

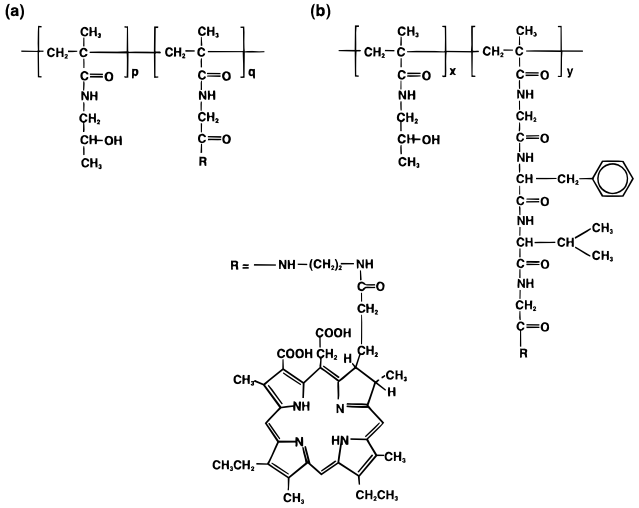

Figure 1. Chemical structure of *N*-(2-hydroxypropyl)methacrylamide (HPMA) copolymer−meso-chlorin e_6 monoethylenediamine conjugates with amino acid (G) (a) or tetrapeptide (GFLG) (b) side chains where R is Mce$_6$.

continuous variation.[23] In brief, two stock solutions were prepared. The first solution contained the free or copolymer-bound Mce$_6$ sensitizers plus the quencher KI. The second one was identical except that the KI was replaced by KCl to keep the ionic strength constant. The desired concentration of KI in solution was obtained by mixing the first solution with the second one. All solutions were prepared shortly before the measurements and stored in the dark. A small amount of 1.0 M thiosulfate was added to the iodide solution (final thiosulfate concentration 10^{-4} M) to prevent the formation of I_3^-, which might influence the effective iodide concentration. The fluorescence was excited at $\lambda = 396$ nm, and the intensity of emitted light was recorded at $\lambda = 650$ nm. The modified Stern−Volmer equation was used to fit the experimental data:

$$\frac{F_0}{F_0 - F} = \frac{1}{K_{SV} f_a Q} + \frac{1}{f_a} \qquad (3)$$

where F and F_0 are the fluorescence intensities in the presence and absence of quencher, respectively. Q is the concentration of quencher, f_a is the fraction of Mce$_6$ species accessible to the quencher, and K_{SV} is the Stern−Volmer collisional quenching constant of this accessible fraction. The f_a and K_{SV} are the only variable parameters in the fitting procedure.

Time-Resolved Fluorescence Decay Measurements. Time-resolved fluorescence decay measurements were performed using an ISS2 K2-FASTSCAN/GREG 200 multifrequency modulation fluorometer. Excitation was provided with an argon laser beam ($\lambda = 514.5$ nm) modulated by a Marconi model 2022A AM/FM signal generator over a frequency range of 10 kHz to 1 GHz. Fluorescence was collected perpendicularly to the excitation beam. The phase shift of the fluorescence signal with respect to the incident signal and its modulation deep was measured as a function of the modulation frequency. Experimental results were analyzed with a model supposing an existence of two fluorescence contributions having different lifetimes.

Results and Discussion

The chemical structures of Mce$_6$ and the various HPMA copolymer−Mce$_6$ conjugates are shown in Figure 1. Since aggregation of Mce$_6$ moieties is medium sensitive[24] and an addition of alcohols and surfactants to aqueous solutions has long been known to disperse dye aggregates,[24−27] the SPB and mixtures of SPB with ethanol and varieties of surfactants were used as solvents. All the data shown are the average of three measurements with errors less than 5%.

1. Dynamic Light Scattering Measurements. The apparent hydrodynamic radii, $R_h^a(90°)$, of the HPMA copolymer−Mce$_6$ conjugates in SPB or ethanol as determined by DLS are given in Table 1. The values for copolymer conjugates **1** and **2** were only slightly larger in SPB than in ethanol, while the values for copolymer conjugates **3** and **4** in SPB were comparable (**3**) or smaller (**4**) than those in ethanol. The relative decrease of $R_h^a(90°)$ in SPB observed for copolymer conjugates **3** and **4** is probably due to side chain hydrophobicity resulting in a partial coil collapse. Since alcohols can efficiently disperse dye aggregates,[24] the inter- and intramolecular aggregation of Mce$_6$ moieties within the copolymer conjugates might be expected to decrease in ethanol. The experimental results that the $R_h^a(90°)$ values of copolymers in SPB are nearly identical with those in ethanol imply that intermolecular aggregation of the copolymers resulting from hydrophobicity of side chains and/or Mce$_6$ moieties is practically negligible. This result is in contrast with the results found in aqueous solutions of Zn(II) phthalocyanine−HPMA copolymer conjugates where a strong random intermolecular association was observed due to the more intensive dimerization of Zn(II) phthalocyanine sensitizers. This suggests that the hydrophobicity of Mce$_6$ molecules is less than that of Zn(II) phthalocyanines.[12,13] Nevertheless, the intramolecular aggregation of Mce$_6$ moieties is not excluded.

2. Absorption Spectra. Indirect evidence for the intramolecular aggregation of Mce$_6$ moieties in SPB was obtained from spectroscopic measurements. The absorption spectra of free Mce$_6$ and Mce$_6$ moieties attached to copolymers as recorded from 300−450 nm (Soret band region) and from 600−700 nm (Q band region) in SPB are given in Figures 2a,b, respectively. The absorption spectrum of free Mce$_6$ molecules showed sharp and more pronounced absorbance peaks in both the Soret and Q bands. Attachment of Mce$_6$ to the HPMA copolymer results in lowering of the absorbance, broadening of both the peaks, and a red shift of the Q band. The more hydrophobic tetrapeptide side chains make all of these effects more pronounced. All of the spectral changes observed, similar to those detected with porphyrins,[25,28] result from an aggregation of the Mce$_6$ species in SPB solutions and they can be attributed to a greater delocalization of π-orbitals (Soret band) in Mce$_6$ aggregates and to a relative intensification of vibrational components of Q bands. The aggregation of Mce$_6$ moieties attached to copolymers is clearly more intensive than the free Mce$_6$ molecules, probably due to a higher local Mce$_6$ concentration in the former case.

The changes of the Soret band spectra of free Mce$_6$ and copolymer conjugates **2** and **4** resulting from the addition of ethanol to SPB (SPB/ethanol mixture solvents) were evaluated by deconvoluting the spectra into two contributing absorbance peaks located at 394 and 374 nm, respectively. The ratio of these two absorbance peak amplitudes, $A(394)/A(374)$, changes from about 2 to 3 as the ethanol content in solvent mixtures increases from 0 to 100 vol % (Figure 3). The ratio is essentially identical ($\approx$3) for free Mce$_6$ molecules and the copolymer conjugates **2** and **4** in 100% ethanol solutions, while significant differences are observed in the SPB solutions. The data at 80 vol % are not shown because the SPB is not completely miscible with ethanol at this volume ratio and a cloudy sample results. Since the addition of ethanol disperses the aggregated Mce$_6$ species,[9,10,24] the $A(394)/A(374)$ ratio can be used as a qualitative measure of the degree of Mce$_6$ monomerization.

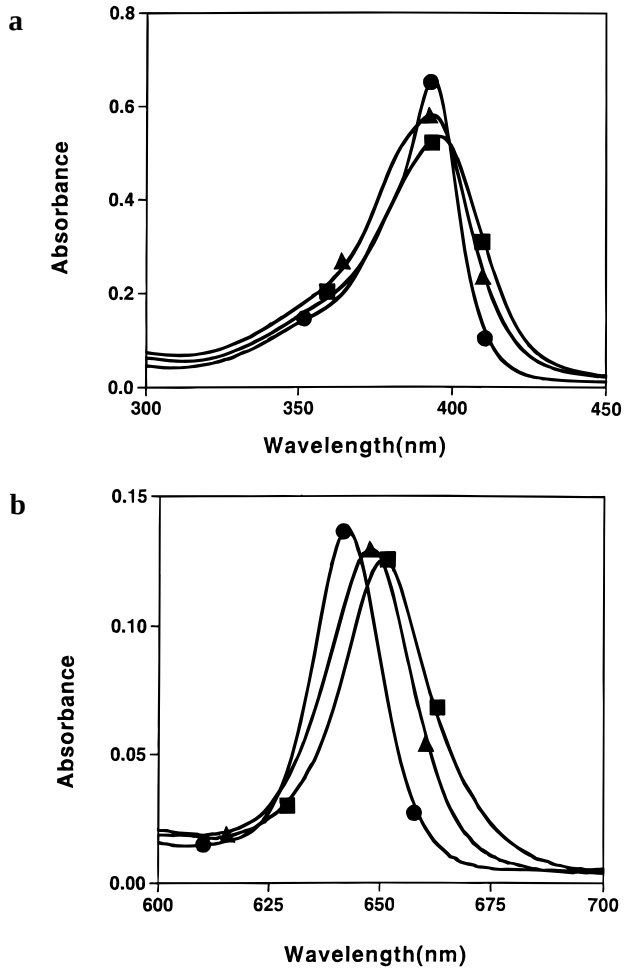

Figure 2. Soret band (a) and Q band (b) absorption spectra of free Mce_6 (●) and copolymer conjugates **2** (▲) and **4** (■) in 20 mM SPB at Mce_6 equivalent concentrations of 5 μM.

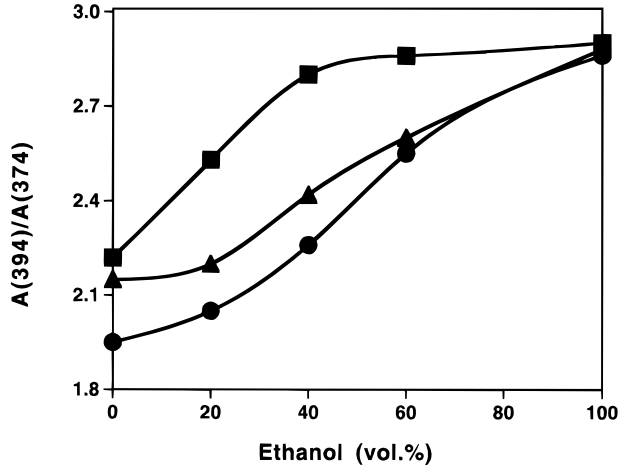

Figure 3. Influence of ethanol contents on the absorbance magnitude ratio of two deconvoluted absorbance peak components located at 394 and 374 nm for free Mce_6 (●) and copolymer conjugates **2** (▲) and **4** (■) at Mce_6 equivalent concentrations of 5 μM.

3. Fluorescence Measurements. The intensity of the fluorescence emitted by the Mce_6 moieties of copolymer conjugate **2** increased progressively as the vol % of ethanol in the solvent increased (Figure 4). This probably results from an increased monomerization of intramolecular Mce_6 aggregates in the conjugate, since it has been shown that the fluorescence efficiency of many photosensitizers is much greater for the monomers than for aggregated species.[29]

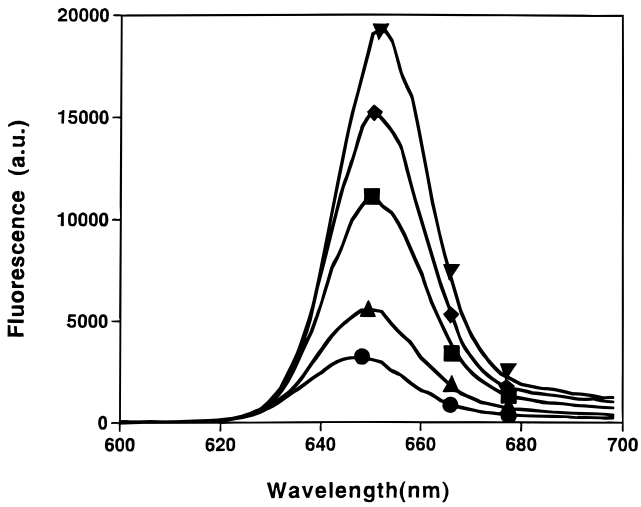

Figure 4. Influence of ethanol contents on the emission spectra of copolymer conjugate **2** at Mce_6 equivalent concentration of 5 μM and λ_{exc} = 394 nm: in sodium phosphate buffer only (●), 20 vol % of ethanol (▲), 40 vol % of ethanol (■), 60 vol % of ethanol (◆), and pure ethanol (▼).

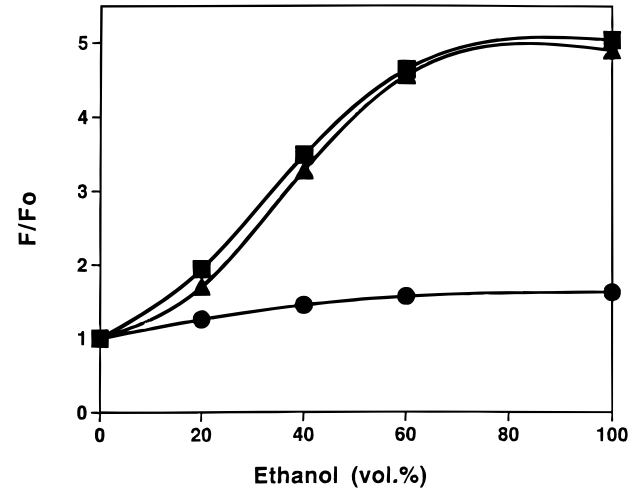

Figure 5. Influence of ethanol contents on the fluorescence intensity in SPB/ethanol mixture solvents for free Mce_6 (●) and copolymer conjugates **2** (▲) and **4** (■) with $\lambda_{exc.}$ = 394 nm and $\lambda_{emi.}$ = 653 nm. F and F_0 are the fluorescence with and without the differential volume addition of ethanol in SPB/ethanol mixture solvents.

The influence of ethanol content on the fluorescence of free Mce_6 and copolymer conjugates **2** and **4** is shown in Figure 5. The fluorescence ratio increased slowly from 1 to 1.5 for free Mce_6, while the ratio increased substantially from 1 to about 5 for copolymer conjugates **2** and **4**. This is not surprising since only a low degree of aggregation exists for free Mce_6 and small fluorescence intesity changes are expected upon the addition of ethanol. On the contrary, the extensively intramolecular aggregation of the copolymer-bound Mce_6 is very sensitive to the thermodynamic quality of the solvent. As expected, addition of ethanol results in the monomerization of Mce_6 with a concomitant large increase of fluorescence intensity. The slightly higher fluorescence ratio of copolymer conjugate **4** than conjugate **2** also may imply the existence of more aggregated Mce_6 species resulting from the more hydrophobic side chains in conjugate **4** since the more aggregated Mce_6 species are shifted to the monomerized Mce_6. This monomerization shift from the more aggregated Mce_6 species in conjugate **4**, compared with the less aggregated Mce_6 species in conjugate **2**, may result in the higher fluorescence ratio.

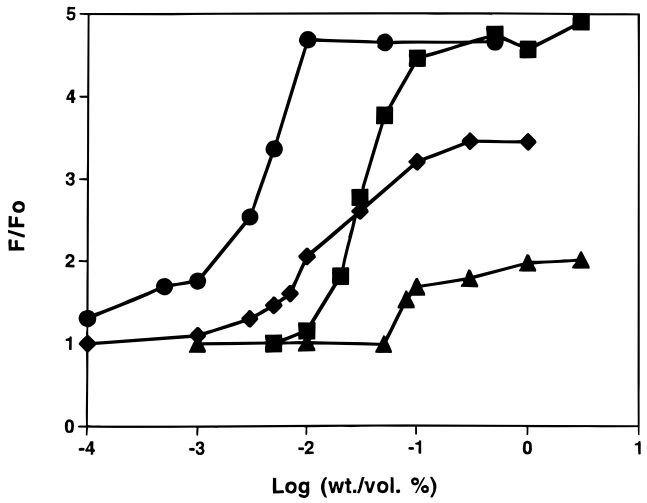

Figure 6. Fluorescence enhancement of copolymer conjugate **2** at an Mce$_6$ equivalent concentration of 5 μM by CTAB (●), SDS (▲), Triton X-100 (■), and HSA (◆). F_0 and F are the fluorescence intensities without and with the addition of detergents or protein, respectively. λ_{exc} = 394 nm and λ_{emi} = 650 nm.

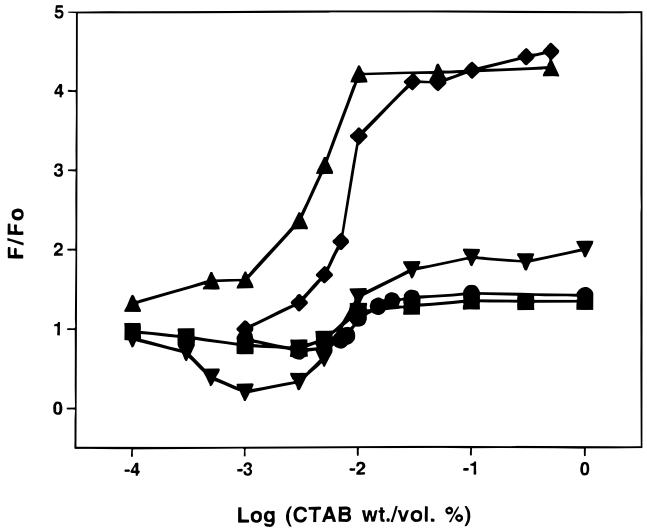

Figure 7. Fluorescence enhancement of free Mce$_6$ (▼), and copolymer conjugates **1** (●), **2** (▲), **3** (■), and **4** (◆) by CTAB at an Mce$_6$ equivalent concentration of 5 μM. F_0 and F are the fluorescence intensities without and with the addition of CTAB, respectively. λ_{exc} = 394 nm and λ_{emi} = 650 nm.

Low molecular weight detergents can also monomerize aggregated Mce$_6$, porphyrins, and other photosensitizers. As shown in Figure 6, the intensity of the Mce$_6$ fluorescence from copolymer conjugate **2** was increased over 4-fold by CTAB and Triton X-100 at concentrations above 0.01 and 0.03 wt/vol %, respectively. SDS was much less efficient; it enhanced fluorescence only 50% at concentrations greater than 0.3 wt/vol %. The increases in intensity occurred at detergent concentrations just above their C_{MC}.

The fluorescence increases produced by the detergents probably result from monomerization of the intramolecular Mce$_6$ aggregates in the copolymer conjugate by interaction with the hydrocarbon chains of the detergent micelles. The different efficiencies of the three detergents probably reflect different types of interactions between the detergents and the Mce$_6$ moieties in the copolymer, which are negatively charged under the reaction conditions used. CTAB (cationic = positively charged) associates closely with Mce$_6$ due to electrostatic forces. In contrast, SDS (anionic = negatively charged) would be electrostatically repulsed by Mce$_6$. With Triton X-100 (nonionic = uncharged), Mce$_6$ aggregates are probably dispersed solely by hydrophobic interactions.

Figure 6 also shows that the fluorescence from conjugate **2** was increased 2−3-fold by human serum albumin (HSA) at concentrations greater than 0.01 wt/vol %. This probably results from the noncovalent attachment of Mce$_6$ moieties within the copolymer conjugate onto the protein. This interaction initiates the conformation changes of the conjugate that break up the intramolecular Mce$_6$ aggregates. This phenomenon has been observed with aggregates of porphyrins in solution. Only monomeric porphyrin binds to the protein, thus shifting the equilibrium of the aggregation reaction to the protein-bound monomeric form, which is much more fluorescent than the aggregated forms.[29]

The effects of CTAB concentration on the fluorescence intensities of Mce$_6$ and of the four HPMA copolymers with different contents of Mce$_6$ (Table 1), as measured in SPB, are shown in Figure 7. The relative fluorescence intensity of free Mce$_6$ decreased, went through a minimum of 0.3 at a CTAB concentration of 10^{-3} wt/vol %, and then increased and leveled off at 1.7 at 0.3 wt/vol % as the concentration of CTAB was increased from 10^{-4} to 1.0 wt/vol %. For copolymer conjugates **1** and **3** (low Mce$_6$ content), the relative intensities went through a minimum of 0.8 and then increased to 1.2 as the CTAB concentration increased. For conjugates **2** and **4** (high Mce$_6$ content), the fluorescence increased to 4.3 and 4.5, respectively. The effect of CTAB on the fluorescence of conjugates **1** and **3** is small, probably because of their low Mce$_6$ loading, which results in less intramolecular aggregation. The large increases with conjugates **2** and **4** could reflect their greater Mce$_6$ loading, which would induce more aggregation. Conjugate **4** had a larger fluorescence ratio than conjugate **2**, probably reflecting an effect of the more hydrophobic amino acid side chain in this copolymer.

The decreased fluorescence of Mce$_6$ observed at CTAB concentrations below the C_{MC} may be best explained by the formation of an electrically neutral Mce$_6$−2 CTAB complex. These would be highly hydrophobic and tend to aggregate more than free Mce$_6$. At CTAB concentrations above the C_{MC}, detergent micelles would form that, in turn, could monomerize the Mce$_6$ aggregates. Similar phenomena have been observed with other photosensitizers, such as eosin Y and Rose bengal.[26]

4. Detergent Effects on Photosensitizing Efficiency. The effects of CTAB, Triton X-100, and SDS concentrations on the quantum yields of oxygen uptake during the photooxidation of furfuryl alcohol by copolymer conjugate **4** were measured. The results, expressed as relative quantum yields ([yields in the presence of detergent]/[yields in the absence of detergent]) are shown in Figure 8. With CTAB, the relative quantum yield increased more than 3-fold with increasing detergent concentrations. Triton X-100 gave similar results, but somewhat higher detergent concentrations were required. The yield initially decreased slightly with increasing SDS concentration and then increased 2-fold at very high detergent concentrations. Thus the relative efficiencies of the different detergents for increasing the photosensitizing efficiency of copolymer conjugate **4** were CTAB > Triton-100 ≫ SDS, the same as for increasing the fluorescence efficiencies of the conjugates.

One mechanism involved in the detergent effect is probably partial dissociation of the intramolecular Mce$_6$ aggregates in the copolymer conjugates. It is well established that aggregation of tetrapyrroles significantly decreases their efficiency in producing singlet oxygen on illumination. Another mechanism could involve changes of the conjugate conformation in such a

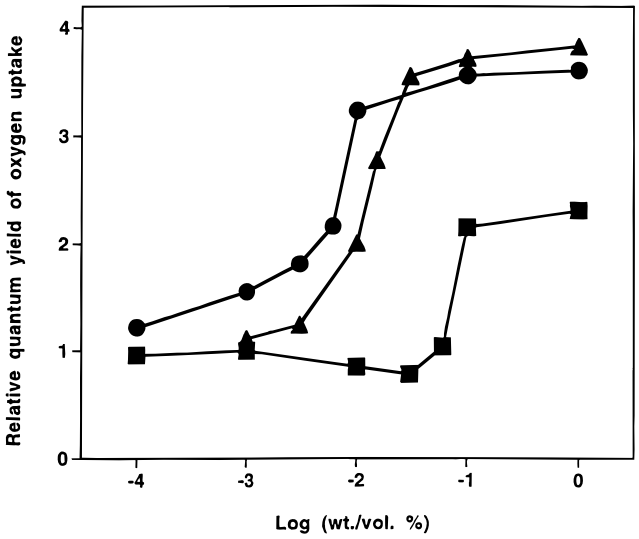

Figure 8. Effects of CTAB (●), Triton X-100 (▲), and SDS (■) concentrations on the relative quantum yields of oxygen uptake during the photooxidation of furfuryl alcohol as sensitized by copolymer conjugate **4**. The reaction mixtures were 20 mM in SPB of pH 7.4, 0.5 mM in furfuryl alcohol, and 0.22 mM in oxygen (air-saturated) and contained copolymer conjugate **4** equivalent to 5 μM Mce_6.

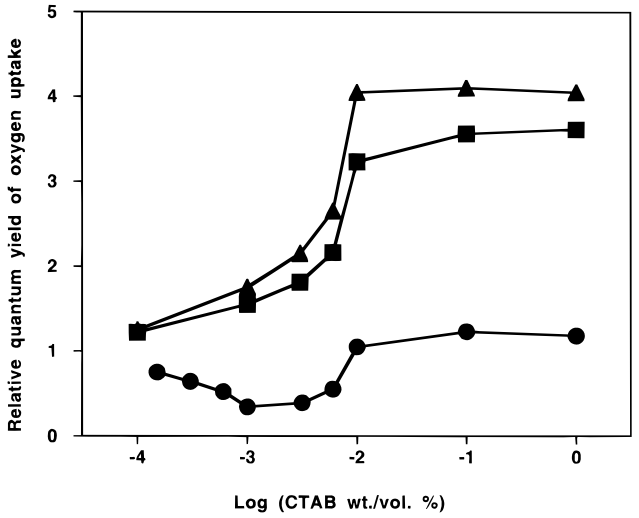

Figure 9. Effects of CTAB concentration on the relative quantum yields of oxygen uptake during the photooxidation of furfuryl alcohol as sensitized by 5 μM Mce_6 (●) and by 5 μM Mce_6 equivalent concentrations of copolymer conjugates **2** (▲) and **4** (■). The other reaction conditions were the same as for Figure 8.

way as to increase the probability of collisional interactions between sensitizer molecules and dissolved oxygen. The different efficiencies of the detergents again probably result from their different electrostatic and/or hydrophobic interactions with the conjugate as described above.

The effects of CTAB concentration on the relative photosensitizing efficiencies of Mce_6 and copolymer conjugates **2** and **4** are shown in Figure 9. With increasing CTAB concentration, the photosensitizing efficiency of free Mce_6 decreased to approximately one-third of that in the absence of detergent and then increased to slightly over the original value at high detergent concentrations. The relative efficiencies increased 4-fold with conjugate **2** and over 3-fold with conjugate **4**. Again, the increased efficiency of singlet oxygen generation by the copolymer conjugates probably results from monomerization of the intramolecular sensitizer aggregates and changes in conjugate conformation.

5. Fluorescence Quenching Measurements. The fluorescence of free Mce_6 and copolymer conjugates **2** and **4** was quenched by the iodide anion in SPB. From eq 3, linear modified Stern−Volmer relationships are obtained with the Stern−Volmer collisional quenching constant $K_{SV} = 4.82$, 4.57, and 4.34 M^{-1}, respectively, and f_a, the fraction available to iodide anion quenching, = 1.0, 0.56, and 0.46 for free Mce_6 and copolymer conjugates **2** and **4**, respectively (all $R^2 > 0.98$) (Figure 10). The lower K_{SV} value indicates that fewer Mce_6 species collide with iodide anions, and a smaller f_a implies that hydrophobic domains formed by aggregation of Mce_6 species may exist in SPB solutions of copolymer conjugates. These hydrophobic domains can arise from attractive (intramolecular) hydrophobic interaction of Mce_6 species inside coils of copolymer conjugates where the local Mce_6 concentration is higher than in the solution. Practically all unbound Mce_6 species were available for iodide quenching in aqueous solutions. It appears that the HPMA copolymer backbone forms a hydrophilic shell surrounding the aggregated hydrophobic Mce_6 species. The formation of molecular micelles renders the Mce_6 moieties less accessible to iodide quenching. The decreased quenching capability of iodide is most visible for copolymer conjugate **4** containing hydrophobic tetrapeptide side chains. Most probably this conjugate forms the most compact micellar cores.

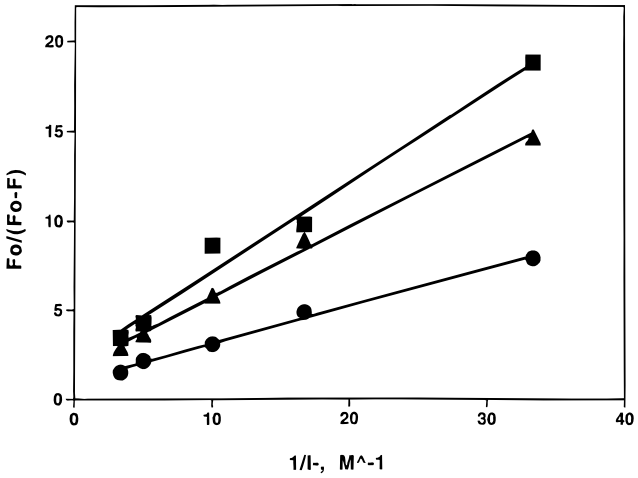

Figure 10. Modified Stern−Volmer plots of free Mce_6 (●) and copolymer conjugates **2** (▲) and **4** (■). The reaction mixtures were 20 mM in SPB of pH 7.4 and 0.22 mM in oxygen (air saturated) and contained 5 μM Mce_6 or 5 μM Mce_6 equivalent concentrations of copolymer conjugates **2** or **4**. Excitation 394 nm, emission 650 nm.

6. Time-Resolved Fluorescence Measurements. The time-resolved fluorescence decays of free Mce_6 and copolymer conjugates **2** and **4** were measured in aqueous SPB and ethanol. The fluorescence of free Mce_6 decayed by a single exponential function of time in both solvents. The fluorescence of the Mce_6 in the copolymer conjugates decayed by a single mode in ethanol. In contrast, the decay in aqueous buffer was more complex but could be resolved into a slow and a fast component. The various fluorescence lifetimes in the two solvents are listed in Table 2. The slow decay lifetimes for free Mce_6 and the two conjugates were very similar; they were also similar and slightly longer in ethanol. The fast decay lifetime of conjugate **2** in ethanol was slightly longer than that of conjugate **4**. From the copolymer conjugate data in buffer, it was calculated that approximately 15% of the fluorescence decayed by the fast mode.

By analogy to measurements with porphyrins[28] and the results of other earlier studies on HPMA copolymer−Mce_6 conjugates,[9,10] the long-lived decay component observed in buffer and in ethanol probably represents fluorescence emission from

TABLE 2: Fluorescence Lifetimes (τ) and Fraction of the Fast Fluorescence Component in Solutions of Free Mce_6 Molecules and HPMA Copolymer−Mce_6 Conjugates, As Measured in 20 mM Sodium Phosphate Buffer of pH 7.4 and in Ethanol

samples	τ_{fast} (ns) buffer/ethanol	τ_{slow} (ns) buffer/ethanol	fr_{fast}[a] buffer/ethanol
Mce_6	ND[b]/ND[b]	4.30/4.90	0/0
2	1.03/ND[b]	4.13/4.72	0.15/0
4	1.17/ND[b]	4.24/4.71	0.14/0

[a] fr_{fast} is the fraction of the fast fluorescence component. [b] Not determinable.

monomeric Mce_6. The short-lived component observed with the copolymer in buffer probably comes from the aggregated Mce_6 species. There are no aggregated species in ethanol, so only the long-lived fluorescence is observed in this solvent. Again, these studies provide evidence for the presence of intramolecular aggregates of the Mce_6 moieties in the copolymer conjugates in SPB.

Conclusions

The objective of this study was to examine the solution and photoproperties of HPMA copolymer−Mce_6 conjugates. From the results of the present study, we can propose a macromolecular conformation for the HPMA copolymer-Mce_6 conjugate in SPB. Dynamic light scattering measurements indicate that the intermolecular aggregation of Mce_6 within copolymer conjugates is not significant. Both absorption and fluorescence spectra confirm the existence of intramolecularly aggregated Mce_6 species. Fluorescence quenching measurements indicate the presence of hydrophobic Mce_6 domains identical with cores of unimer micelles of random copolymers. Fluorescence lifetime measurements also indicate the existence of Mce_6 aggregation. Thus, all experiments seem to indicate that the covalent binding of Mce_6 to HPMA copolymers significantly facilitates the formation of intramolecular Mce_6 aggregates in aqueous solutions. The studies on the influence of the thermodynamic quality of the solvent and of side chain hydrophobicity on the solution properties of the conjugates has shown that (1) the aggregated Mce_6 species are progressively dissociated into monomeric Mce_6 species by increasing the vol % of ethanol in the solution, (2) the degree of aggregation is lower in SPB solutions of free Mce_6 molecules than in solutions of copolymer Mce_6 conjugates, and (3) the more hydrophobic GFLG side chains facilitate the aggregation of Mce_6 within the copolymer conjugate in SPB.

Acknowledgment. We thank Drs. P. Kopečková, V. Omelyanenko, and V. Hlady for valuable discussions and Ms. Pat Meekins for skillful technical assistance. This research was supported in part by the NIH National Cancer Institute (Grant CA 51578), the U.S.-Czechoslovak Science and Technology Program (No. 93003) and the Grant Agency of the Academy of Sciences of the Czech Republic (No. 307/96/K226).

References and Notes

(1) van Lier, J. E. In *Photodynamic Therapy of Neoplastic Disease*; Kessel, D., Ed.; CRC Press: Boca Raton, FL, 1990; Vol. I.
(2) Putnam, D.; Kopeček, J. *Adv. Polym. Sci.* **1995**, *122*, 55.
(3) Bader, H.; Ringsdorf, H.; Schmidt, B. *Angew. Makromol. Chem.* **1984**, *123/124*, 457.
(4) Ulbrich, K.; Koňák, Č.; Tuzar, Z.; Kopeček, J. *Makromol. Chem.* **1987**, *188*, 1261.
(5) Nukui, M.; Hoes, K.; van den Berg, H.; Feijen, J. *Makromol. Chem.* **1991**, *192*, 2925.
(6) Ambler, E. L.; Brookman, L.; Brown, J.; Goddart, P.; Petrak, K. *J. Bioact. Comp. Polym.* **1992**, *7*, 223.
(7) Koňák, Č.; Rathi, R. C.; Kopečková, P.; Kopeček, J. *Polymer* **1993**, *34*, 4767.
(8) Koňák, Č.; Kopečková, P.; Kopeček, J. *Macromolecules* **1992**, *25*, 5451.
(9) Krinick, N. L.; Sun, Y.; Joyner, D.; Spikes, J. D.; Straight, R. C.; Kopeček, J. *J. Biomater. Sci., Polym. Ed.* **1994**, *5*, 303.
(10) Spikes, J. D.; Krinick, N. L.; Kopeček, J. *J. Photochem. Photobiol. A: Chem.* **1993**, *70*, 163.
(11) Kiserow, D. J.; Itoh, Y.; Webber, S. E. *Macromolecules* **1996**, *29*, 7847.
(12) Gu, Z.-W.; Spikes, J. D.; Kopečková, P.; Kopeček, J. *Collect. Czech. Chem. Commun.* **1993**, *58*, 2321.
(13) Gu, Z.-W.; Koňák, Č.; Kopečková, P.; Kopeček, J. *Macromolecules* **1995**, *28*, 8375.
(14) Wöhrle, D.; Krawczyk, G. *Makromol. Chem.* **1986**, *187*, 2535.
(15) Krinick, N. L.; Sun, Y.; Joyner, D. A.; Reed, R.; Spikes, J. D.; Straight, R. C.; Kopeček, J. *Proc. Soc. Photo-opt. Instrum. Eng.* **1992**, *1645*, 142.
(16) Kopeček, J.; Rejmanová, P.; Strohalm, J.; Ulbrich, K.; Říhová, B.; Chytrý, V.; Lloyd, J. B.; Duncan, R. U.S. Patent 5,037,883, August 6, 1991.
(17) Strohalm, J.; Kopeček, J. *Angew. Makromol. Chem.* **1978**, *70*, 109.
(18) Yen, H.-R.; Kopeček, J.; Andrade, J. D. *Makromol. Chem.* **1989**, *190*, 69.
(19) Rejmanová, P.; Labský, J.; Kopeček, J. *Makromol. Chem.* **1977**, *178*, 2159.
(20) Reddi, M. A.; Rodgers, J.; Spikes, J. D.; Jori, G. *Photochem. Photobiol.* **1984**, *40*, 415.
(21) Haag, W. R.; Hoigne, J.; Gassman, E.; Braun, A. M. *Chemosphere* **1984**, *13*, 631.
(22) Maurette, M.-T.; Oliveros, E.; Infelta, P. P.; Ramsteiner, K.; Braun, A. M. *Helv. Chim. Acta* **1983**, *66*, 722.
(23) Maurice, R. E. In *Biophysical and Biochemical Aspects of Fluorescence Spectroscopy*; Dewey, T. G., Ed.; Plenum Press: New York, 1995; Chapter 1.
(24) Spikes, J. D.; Bommer, J. C. *Photochem. Photobiol.* **1993**, *17*, 135.
(25) White, W. I. In *The Porphyrins*; Dolphin, D., Ed.; Academic Press: New York, 1978; Vol. V, Chapter 7, pp 303−339.
(26) Bilski, P.; Dabestani, R.; Chignell, C. F. *J. Phys. Chem.* **1991**, *95*, 5784.
(27) Tanielian, C.; Henrich, G. *Photochem. Photobiol.* **1995**, *61*, 131.
(28) Reddi, E.; Jori, G. *Rev. Chem. Intermed.* **1988**, *10*, 241.
(29) Cohen, S.; Margalit, R. *Biochem. J.* **1990**, *270*, 325.